**Author(s):** Tuononen, Heikki; Roesler, Roland; Dutton, Jason; Ragogna, Paul

**Title:** Electronic Structures of Main-Group Carbene Analogues

**Year:** 2007

**Version:**

**Please cite the original version:**

Tuononen, H., Roesler, R., Dutton, J., & Ragogna, P. (2007). Electronic Structures of Main-Group Carbene Analogues. Inorganic Chemistry, 46(25), 10693-10706. https://doi.org/10.1021/ic701350e

**Electronic Structures of Main Group Carbene Analogues**

Heikki M. Tuononen,[§,*] Roland Roesler,[†] Jason L. Dutton,[‡] and Paul J. Ragogna[‡]

*Contribution from the Department of Chemistry, University of Jyväskylä, P.O. Box 35, FI-40014 Jyväskylä, Finland, Department of Chemistry, University of Calgary, 2500 University Dr. NW, Calgary, Alberta, T2N 1N4 Canada, and Department of Chemistry, University of Western Ontario, London, Ontario, N6A 5B7 Canada*

The electronic structures of fifteen Group 13-16 carbene analogues are analyzed using various quantum chemical methods and compared to the data obtained for the parent *N*-heterocylic carbene (NHC), imidazol-2-ylidene. The results of this study present a uniform analysis of the similarities and differences in the electronic structures of p-block main group carbene analogues. Though all systems are formally isovalent, the theoretical analyses unambiguously indicate that their electronic structures run the gamut from C=C localized (Group 13) to C=N localized (Group 16) via intermediate, more delocalized, systems. In particular, neither the stibenium ion nor any of the chalcogenium dications is a direct analogue of imidazol-2-ylidene as they all contain two lone pairs of electrons around the divalent main group center, instead of the expected one. The reason behind the gradual change in the electronic structure of main group analogues of imidazol-2-ylidene was traced to the total charge of the systems, which changes from anionic to dicationic when moving from left to right in the periodic table. Results from theoretical analyses of aromaticity show that all Group 13-16 analogues of imidazol-2-ylidene display some degree of aromatic character. The heavier Group 13 anions benefit the least from π-electron delocalization, whereas the cationic Group 15 systems are on par with the parent carbon system and display only slightly less aromatic character than cyclopentadienide, a true 6π-electron aromatic species. The σ-donor and π-acceptor ability of the different main group carbene analogues is also evaluated.

[*] Author to whom correspondence should be addressed. E-mail: hetuonon@jyu.fi

[§] University of Jyväskylä

[†] University of Calgary

[‡] University of Western Ontario

## Introduction

Carbenes are compounds with a neutral divalent carbon atom with only six electrons in its valence shell. These compounds have played a major role in several fields of chemistry[1] ever since their existence was first confirmed.[2] As excellent σ-donors, carbenes can substitute classical two-electron donor ligands such as amines, ethers, and phosphanes in coordination chemistry. Hence, coupled with transition metals, carbenes have lead to organometallic catalysts with enormous potential in numerous chemical applications.[1d,3] Carbenes have also attracted interest as reagents in organic transformations (*e.g.* transesterification, nucleophilic aromatic substitution, and cycloaddition chemistry).[4] Some of the latest developments in carbene chemistry include their use in highly specific functions such as antimicrobial agents[5] and in liquid crystals,[6] and further investigations will undoubtedly reveal many more fascinating and useful applications for these systems as a whole.

The imidazol-2-ylidenes and other *N*-heterocyclic carbenes (NHCs) containing two amino fragments are the most studied and well-understood of the carbenes since they are the most stable derivatives known to date.[2] The intrinsic instability of a neutral divalent carbon is perhaps best illustrated by the fact that 30 years elapsed between the initial reports on NHCs and the isolation and complete characterization of the first bottleable derivative.[2] In recent years, it has been shown that the backbones of NHCs can be significantly modified without diminishing their stability and examples of saturated[7] and acyclic[8] carbenes, and NHCs with four-, six-, and seven-membered rings have been reported;[9] the first example of a stable carbene which remarkably lacks π-donor heteroatoms has also been published.[10] In addition, there have been extensive efforts to isolate and characterize the isovalent p-block analogues of imidazol-2-ylidene, collectively known as the main group carbene analogues. These compounds have been successfully synthesized for many elements from Groups 13 to 16:[11] in each case, the main group centre is dicoordinate, electron rich (bears a

lone pair of electrons), and formally anionic (Group 13), neutral (Group 14), cationic (Group 15), or dicationic (Group 16).

Due to their important role in different chemical applications, NHCs have gathered a significant amount of computational interest. Numerous theoretical reports which discuss the electronic structures and properties of the free ligands[12] or bonding and reactivities of their various transition metal complexes have been published.[13] This has provided tremendous insight to the whole field of NHC chemistry. For example, the exceptional stability of NHCs, which at first was attributed to a combination of σ-bonding effects and the use of bulky substituents,[14] was shown to arise primarily from the delocalization of π-electrons throughout the NCN framework with the help of detailed theoretical calculations and electronic structure analyses.[15] As this stabilizing contribution is present in all types of NHCs, the results also provided rationalization for the isolation of both saturated and acyclic systems. Hence, over the years computational studies have provided important information about NHCs which would have been difficult, or in some cases impossible, to obtain by any other means.

Significantly less is known about the electronic structures of main group carbene analogues than of the parent carbon system. In particular, one of the key questions that has not yet been thoroughly answered is to what extent the different p-block imidazol-2-ylidene analogues mimic the electronic structure and properties of NHCs. While in-depth theoretical studies have been conducted for silylenes and germylenes,[15,16] as well as phosphenium cations,[17] only a few publications analyzing the electronic structures of Group 13[18] or the heaviest Group 14[11f] and 15[17d] carbene analogues exist. In addition, no more than an initial report of the electronic structures of the dicationic Group 16 carbene analogues has been presented due to their very recent discovery.[11k] In addition, the published computational studies represent a heterogeneous mixture of different methods and tools which hinders simple comparison of results obtained for different systems. The diverse nature of the theoretical results, or the lack of thereof, has also lead to some interesting and

sometimes conflicting claims. For example, total consensus about the significance of π-electron delocalization in Group 15 carbene analogues has not yet been reached: while magnetic properties and energetic analyses have indicated a high degree of aromatic stabilization,[17] some authors have argued in favor of localized electronic structures based on the trends in determined metrical parameters.[11i] Another interesting detail in the chemistry of main group carbene analogues is highlighted by the electronic structure of the tin analogue of imidazol-2-ylidene which has been described by a chelate-type model **I** containing the dicoordinate Group 14 element in a rather atypical formal oxidation state zero;[11f] the importance of this resonance contributor has also been discussed in context of systems **6** and **7**.[16b]

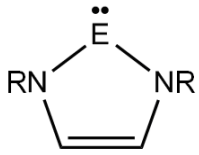


**1: E = $B^-$** **5: E = C** **9: E = $N^+$** **13: E = $O^{2+}$**
**2: E = $Al^-$** **6: E = Si** **10: E = $P^+$** **14: E = $S^{2+}$**
**3: E = $Ga^-$** **7: E = Ge** **11: E = $As^+$** **15: E = $Se^{2+}$**
**4: E = $In^-$** **8: E = Sn** **12: E = $Sb^+$** **16: E = $Te^{2+}$**

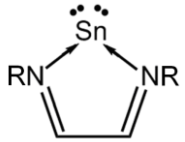


**I**

In this contribution, we present the first systematic computational analysis of 15 Group 13-16 analogues of imidazol-2-ylidene, **1**-**4** and **6**-**16**. The parent carbon species **5** has been extensively studied in the past and is included only as a benchmark to facilitate direct comparison of different systems. The primary aim of this study is to find accurate yet simple descriptions of the electronic structures of different main group carbene analogues. Aromatic stabilization in **1**-**16** is probed from multiple perspectives (electronic, energetic, and magnetic) in order to obtain information regarding the extent of π-electron delocalization in different systems. The influence of the dicoordinate center E on the bonding properties of the free ligands, especially in the context of NHCs as π-acceptors, is

also discussed. All of the above goals will be reached using density functional theory (DFT) calculations coupled with different electron density analysis methods.

## Computational Details

Molecular geometries of **1**-**16** were optimized with DFT using the PBE1PBE exchange-correlation functional[19] with Ahlrichs' TZVP basis sets;[20a] the corresponding ECP basis sets were used for the heavy Period 5 nuclei In, Sn, Sb, and Te.[20b] All calculations were performed with Gaussian 03.[21] Natural atomic orbital and natural bonding orbital analyses were conducted using the NBO 5.0 code[22] and electron localization function analyses were performed with the program package TopMod.[23] Program Bubble[24] was used in atoms-in-molecules analyses to locate the [3,–3] critical points from the Laplacian of the electron density of Group 13 anions **1**-**4**.

Geometry optimizations were conducted for *N*-H, *N*-Me, and *N*-Ph substituted structures; the bond parameter data reported in Table 1 are for the Ph-substituted derivatives. The results from orbital and electron density analyses are, however, reported only for the H-substituted structures because of two primary reasons. (i) The results from different analyses were found to be largely independent of the identity of the substituent attached to the nitrogen atoms. (ii) The visualization and interpretation of results is greatly simplified if structures with hydrogen substituents are used in the analysis.

## Results and Discussion

**Molecular Geometries.** Table 1 lists the optimized metric parameters of **1**-**16** along with average experimental values determined for a variety of their substituted analogues.[11] As a whole, the calculated bond angles and bond lengths are in good agreement with the values determined by X-ray crystallography when the different electronic and steric effects present in the experimentally characterized systems due to *N*,*N*-substitution are taken into account. As expected, all calculated

structures show perfectly planar geometries. The structures of the five-membered ring resemble that of a regular pentagon when E is any of the Group 13-16 elements from the second row, but distort significantly from the *pseudo*-$C_5$ axis, as the two EN bonds lengthen and the NEN angle becomes more acute for systems containing the heavier p-block elements (n ≥ 3).

**Table 1.** Calculated and Experimental Metrical Parameters of Ph-substituted Systems **1**-**16**[a,b]

| | *r(EN)* | *r(NC)* | *r(CC)* | *∠NEN* | *∠ENC* | *∠NCC* |
|---|---|---|---|---|---|---|
| ***1***; *E* = $B^-$ | *1.502* [1.466] | *1.393* [1.398] | *1.344* [1.326] | *98.0* [99.2] | *111.6* [111.0] | *109.4* [109.0] |
| ***2***; *E* = $Al^-$ | *1.969* | *1.385* | *1.348* | *82.8* | *111.5* | *117.0* |
| ***3***; *E* = $Ga^-$ | *2.049* [1.970] | *1.380* [1.409] | *1.350* [1.374] | *80.6* [83.0] | *111.6* [119.7] | *118.1* [115.9] |
| ***4***; *E* = $In^-$ | *2.243* | *1.378* | *1.353* | *76.1* | *111.1* | *120.8* |
| ***5***; *E* = *C* | *1.361* [1.368] | *1.389* [1.388] | *1.345* [1.338] | *102.1* [101.9] | *112.8* [112.7] | *106.2* [106.4] |
| ***6***; *E* = *Si* | *1.789* [1.750] | *1.382* [1.386] | *1.347* [1.335] | *86.0* [88.4] | *113.8* [112.3] | *113.2* [113.5] |
| ***7***; *E* = *Ge* | *1.894* [1.856] | *1.376* [1.384] | *1.351* [1.364] | *83.0* [84.8] | *113.6* [113.3] | *114.9* [114.3] |
| ***8***; *E* = *Sn* | *2.073* [2.093] | *1.372* [1.378] | *1.354* [1.356] | *78.3* [77.6] | *113.4* [113.5] | *117.4* [113.8] |
| ***9***; *E* = $N^+$ | *1.309* [1.318] | *1.357* [1.345] | *1.362* [1.355] | *105.1* [103.8] | *112.2* [112.6] | *105.3* [105.6] |
| ***10***; *E* = $P^+$ | *1.697* [1.651] | *1.358* [1.368] | *1.363* [1.343] | *88.5* [90.1] | *114.1* [113.6] | *111.7* [111.3] |
| ***11***; *E* = $As^+$ | *1.829* [1.816] | *1.349* [1.359] | *1.370* [1.362] | *84.3* [85.2] | *114.1* [113.6] | *113.7* [113.8] |
| ***12***; *E* = $Sb^+$ | *2.014* [2.022] | *1.345* [1.354] | *1.375* [1.363] | *77.9* [79.6] | *114.4* [113.3] | *116.2* [116.9] |
| ***13***; *E* = $O^{2+}$ | *1.369* | *1.322* | *1.390* | *105.9* | *109.5* | *107.5* |
| ***14***; *E* = $S^{2+}$ | *1.705* | *1.331* | *1.389* | *90.3* | *112.0* | *112.8* |
| ***15***; *E* = $Se^{2+}$ | *1.849* [1.890] | *1.325* [1.293] | *1.394* [1.415] | *85.5* [81.8] | *112.3* [114.9] | *114.9* [114.2] |
| ***16***; *E* = $Te^{2+}$ | *2.032* | *1.321* | *1.402* | *79.7* | *113.3* | *116.8* |

[a] Average experimental values are taken from reference 11 and reported in square brackets.
[b] Bond lengths are reported in Ångströms (Å) and bond angles in degrees (°).

The bonding in **1**-**16** can be examined more thoroughly by comparing the calculated EN, NC, and CC bond lengths listed in Table 1 with typical values for respective single and double bonds. It becomes immediately evident that the EN bonds in **1**-**16** differ markedly from their representative single bond length values only in structures which incorporate the lightest Group 13-16 elements B to O. Both the NC and CC bonds also show some interesting variations with respect to the identity of the element E. Although all numeric values range between those of single and double bonds, the NC bonds tend to shorten when going down the group or from left to right in the periodic table, whereas the CC bonds behave in the opposite manner. Hence, bonding within the NCCN moiety appears to change gradually from what is mostly an N–C=C–N type structure (Group 13 and 14 systems) to a distinct N=C–C=N bonding arrangement (Group 16 structures). Group 15 cations **8**-**11** seem to fall in between these two alternatives with both the CC and CN bond lengths close to their representative values in aromatic compounds (1.40 Å and 1.34 Å, respectively), which suggests significant delocalization of π-electrons within the NCCN moiety in these compounds.

**Molecular Orbitals.** The π-symmetric valence molecular orbitals (MOs) of **1**-**16** are shown in Figure 1; figures of all valence orbitals of **1**-**16** are included as Supporting Information.

Although all orbital sets appear to be more or less identical, a detailed comparison reveals that some clear trends exist (see Figure 1 and Supporting Information). For example, the contribution from the atomic orbitals (AOs) of the element E to the σ-symmetric MOs generally diminishes going down the group and increases moving from left to right across a period. These changes mirror the differences in both electronegativity and AO energies of the elements E, and indicate that the EN bonds are most ionic and most covalent for main group carbene analogues with heavier (In to Te) and lighter elements (B to O), respectively.

A further trend in the σ-symmetric valence orbitals relates to the shape and number of lone pair-type orbitals on the divalent element E. In Group 13 and 14 systems **1**-**8**, the σ-symmetric lone pair-type orbital is high in energy, centered on the element E and has the expected orbital

morphology. However, the situation is rather different for the Group 16 dications **13-16** which all exhibit two diffuse, low-energy σ-symmetric lone pair-type orbitals. Group 15 analogues of imidazol-2-ylidene fall in between these two cases, showing only one lone pair-type orbital which becomes spatially diffuse and decreases in energy when going down the group.

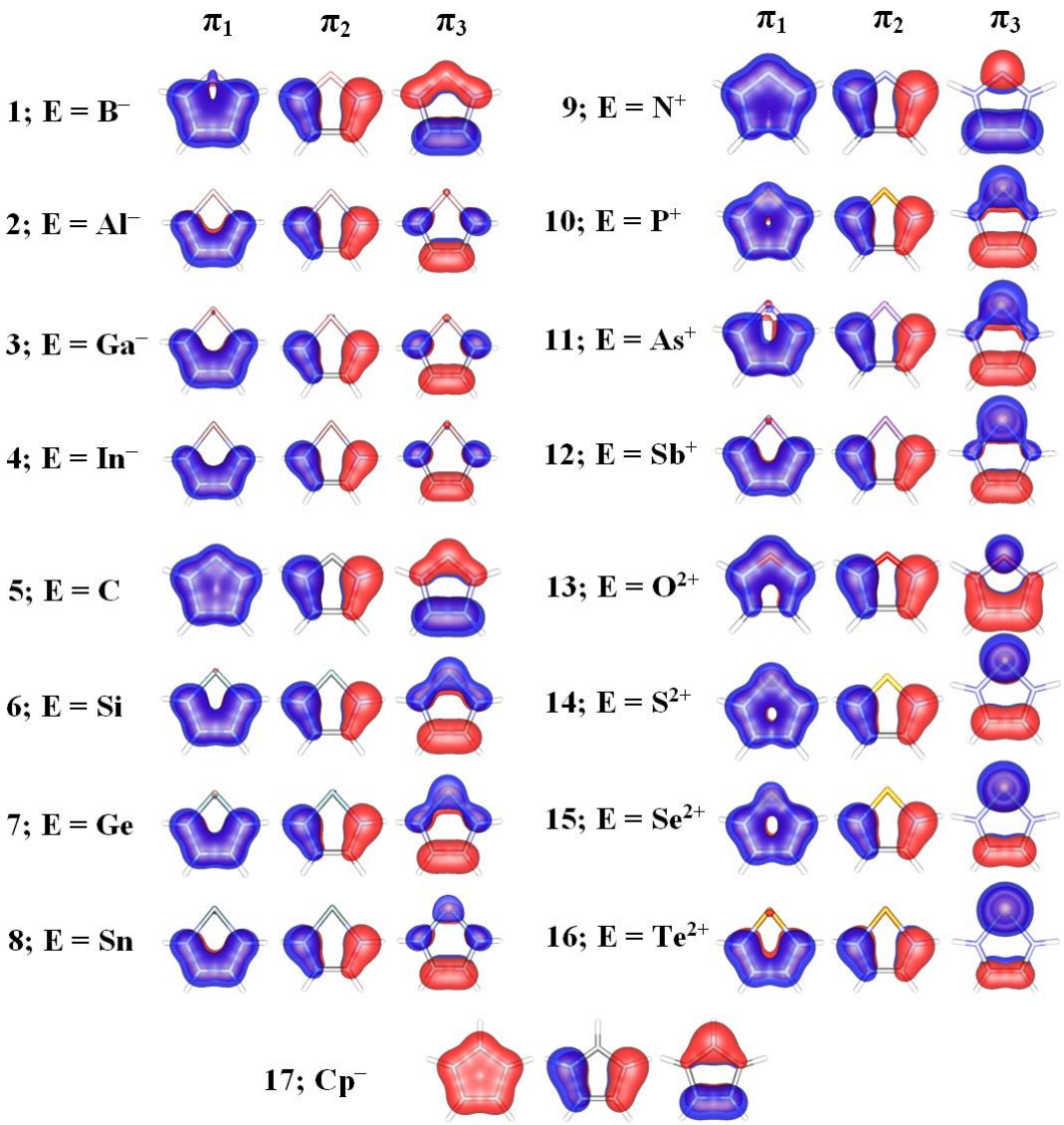


**Figure 1.** π-Symmetric valence molecular orbitals of **1-17**.

The π-symmetric MOs of **1-16** also display some important features which can be used in the qualitative evaluation of the degree of aromatic delocalization in these systems. To this end, it is informative to compare the π orbital sets of **1-16** to the π-system of a well-known isovalent aromatic compound, cyclopentadienide (**17**) ($Cp^-$ in Figure 1). When such comparison is made, it

becomes evident that all systems **1**-**16** display visible similarities with **17** and are thus expected to show some degree of π-delocalization in their ring systems. The most notable differences in the MOs of NHC-type structures as compared to those of cyclopentadienide are the separation of energy levels for $\pi_2$ and $\pi_3$ orbitals as well as the uneven distribution of electron density in $\pi_1$ and $\pi_3$ orbitals. Both changes arise naturally from the introduction of heteroatoms N and E to the all-carbon framework of cyclopentadienide.

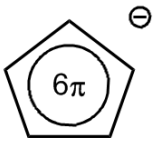


**17**

As shown in Figure 1, all of the heavier Group 13 analogues of imidazol-2-ylidene display a significantly reduced $p_\pi$ orbital overlap in the NEN fragment than that observed for the $\pi_3$ orbitals of the carbon system **5**. The same also applies to the heavier Group 14 NHC analogues, though the effect is notably smaller. The preference of these systems to adopt an N–C=C–N type bonding arrangement is readily explained by the double occupancy of the $\pi_3$ MO which, in essence, contains the CC-bonding-NC-anti-bonding LUMO of a free *cis*-diazabutadiene (*cis*-DAB) ligand. The $\pi_1$ orbitals of **1**-**4** and **6**-**8** show that delocalization of electrons in these systems does not extend significantly beyond the NCCN moiety. Only in the parent NHC is there a significant contribution from the $p_\pi$ orbital of the divalent element E to the $\pi_1$ bonding MO. A more detailed analysis of the π-symmetric MOs of **1**-**8** further reveals that the π-electron density in CC and NC bonds diminishes and increases, respectively, with increasing atomic number of the element E, in good agreement with the observed trends in the calculated metrical parameters.

For the Group 15 and 16 carbene analogues, the constructive $p_\pi$ orbital overlap in the $\pi_1$ bonding MO is substantial and extends over the entire ring even in the phosphenium and selenenium species. Thus, these systems can be expected to display strong diatropic ring currents and, along with the parent NHC, benefit the most from aromatic stabilization. The $\pi_3$ orbitals of **9**-

**16** show a pronounced accumulation of electron density around the element E, which has a significant impact on bonding especially in Group 16 systems. In all chalcogenium dications, the $\pi_3$ MO is either bonding (**13**) or non-bonding (**14-16**) along the NC linkages, whereas the same orbital is predominantly anti-bonding in nature in **1-8**. As the bond parameters of the NCCN moiety mirror the gradual changes in MO characteristics, the above leads to the observed change in NC and CC bonding in Group 16 carbene analogues **13-16** as compared to systems **1-12**. A natural question which immediately follows is whether there exists a simple explanation which would rationalize such a change.

Since all systems **1-16** are formally isovalent, the most obvious culprit for the observed changes in their π-framework is the total charge: when moving from Group 13 to Group 16 systems, the formal charge in the divalent element E changes from monoanionic to dicationic. However, the actual charge distribution in **1-16** differs greatly from the formal one. Table 2 lists the calculated Mulliken and atomic polar tensor (APT) charges for **1-16**. As seen from the numbers, the negative charge in Group 13 carbene analogues **1-4** is spread equally between the element E and the *cis*-DAB ligand only in the boron derivative **1**. In all other Group 13 anions the negative charge is more localized on the DAB ligand. Thus, it is only the boron carbene analogue whose $\pi_1$ and $\pi_3$ orbitals have major contributions from all elements in the five-membered ring. In all of the heavier Group 13 systems, the contribution from the AOs of the element E to the π orbitals is almost nonexistent, which is a consequence of the localization of the negative charge on the DAB ligand.

Analysis of partial charges and MOs calculated for **5-16** shows that the above reasoning also holds for Group 14 systems and, to a lesser extent, for Group 15 carbene analogues. In heavier Group 15 species **10-12**, most of the positive charge is located on the element E, but the difference in charge between the DAB ligand and the Group 15 element remains relatively small. This manifests itself as an increase in the element E contribution to the $\pi_1$ and $\pi_3$ orbitals, and, therefore, in an augmented N=C contribution to π-bonding. The dicationic charge in the Group 16 analogues

of imidazol-2-ylidene suffices to create a totally reversed charge distribution for **13-16**, in which the majority of the positive charge is now located on the *cis*-DAB ligand. This increases the contribution of the AOs from the chalcogen atom to the π-symmetric MOs significantly, bringing about the observed changes in the nodal structure of the $\pi_3$ orbital and in overall π-bonding within the NCCN moiety.

**Table 2.** Mulliken (top) and Atom Polar Tensor (bottom) Charges of **1-16**

| | *δE* | *δN* | *δC* | *δDAB* |
|---|---|---|---|---|
| ***1***; *E* = $B^-$ | *–0.49* | *–0.32* | *–0.14* | *–0.51* |
| | *–0.39* | *–0.44* | *0.00* | *–0.61* |
| ***2***; *E* = $Al^-$ | *–0.22* | *–0.44* | *–0.14* | *–0.78* |
| | *–0.04* | *–0.56* | *0.00* | *–0.96* |
| ***3***; *E* = $Ga^-$ | *–0.14* | *–0.48* | *–0.12* | *–0.86* |
| | *0.11* | *–0.59* | *–0.01* | *–1.11* |
| ***4***; *E* = $In^-$ | *–0.09* | *–0.51* | *–0.12* | *–0.91* |
| | *0.11* | *–0.52* | *–0.07* | *–1.11* |
| ***5***; *E* = *C* | *–0.23* | *–0.15* | *–0.12* | *0.23* |
| | *–0.08* | *–0.28* | *0.00* | *0.08* |
| ***6***; *E* = *Si* | *0.21* | *–0.37* | *–0.09* | *–0.21* |
| | *0.43* | *–0.46* | *–0.03* | *–0.43* |
| ***7***; *E* = *Ge* | *0.35* | *–0.46* | *–0.07* | *–0.35* |
| | *0.49* | *–0.46* | *–0.05* | *–0.49* |
| ***8***; *E* = *Sn* | *0.41* | *–0.48* | *–0.07* | *–0.41* |
| | *0.54* | *–0.41* | *–0.10* | *–0.54* |
| ***9***; *E* = $N^+$ | *–0.03* | *0.02* | *–0.05* | *1.03* |
| | *–0.04* | *–0.05* | *0.03* | *1.04* |
| ***10***; *E* = $P^+$ | *0.53* | *–0.28* | *–0.02* | *0.47* |
| | *0.57* | *–0.22* | *–0.04* | *0.43* |
| ***11***; *E* = $As^+$ | *0.65* | *–0.35* | *0.00* | *0.35* |
| | *0.64* | *–0.21* | *–0.07* | *0.36* |
| ***12***; *E* = $Sb^+$ | *0.71* | *–0.34* | *0.00* | *0.29* |
| | *0.76* | *–0.19* | *–0.11* | *0.24* |
| ***13***; *E* = $O^{2+}$ | *0.19* | *0.09* | *0.10* | *1.81* |
| | *–0.09* | *0.11* | *0.18* | *2.09* |
| ***14***; *E* = $S^{2+}$ | *0.71* | *–0.15* | *0.09* | *1.29* |
| | *0.61* | *–0.06* | *0.07* | *1.39* |
| ***15***; *E* = $Se^{2+}$ | *0.82* | *–0.18* | *0.10* | *1.18* |
| | *0.77* | *–0.07* | *0.04* | *1.23* |
| ***16***; *E* = $Te^{2+}$ | *1.00* | *–0.29* | *0.14* | *1.00* |
| | *0.94* | *–0.08* | *0.00* | *1.06* |

Taken together, the σ and π MO characteristics in **1**-**16** indicate that when moving from Group 13 to Group 16 systems, the lone pair electron density around the divalent element E increases considerably. This is especially true for the chalcogenium species, which in addition to the σ-symmetric lone pair-type orbitals discussed above, show the presence of one π-symmetric MO localized mainly on the chalcogen atom. Such result indicates that the Group 16 systems **14**-**16** contain the chalcogen atom in a formal oxidation state +II (-II for the oxygen analogue **13**) rather than in the expected +IV (0) state and are not Group 16 analogues of the parent imidazol-2-ylidene in the strictest sense.[11k] We note here that the gradual emergence of a lone pair-type $p_\pi$ orbital has already been noted in the literature in the context of Group 14 systems.[11f,16b] The implication of this feature to the electronic structures of **1**-**16** is discussed in detail along with the results from NAO and NBO analyses (see below).

It is instructive to summarize the current findings regarding the aromaticity in **1**-**16** before discussing the results of various bonding analyses any further. If one had to estimate aromatic character in **1**-**16** using MOs alone, the most obvious candidates for having the greatest aromatic stabilization would be the parent NHC as well as its nitrenium and phosphenium analogues because they show MO characteristics which agree best with the π orbitals of cyclopentadienide. Group 16 carbene analogues also show efficient electron delocalization in $\pi_1$ orbitals, but their aromatic nature is probably diminished to some extent by the nodal structure in their $\pi_3$ MOs. It should, however, be noted that even though not all of the Group 13-16 analogues of **5** display efficient π-delocalization throughout the entire five-membered ring, all systems show a varying amount of electron delocalization within the NCCN moiety. This observation readily explains the somewhat unexpected results reported recently for the germylene and silylene species:[25] the experimentally observed depletion of π-electron density in the CC bond of the germylene as compared to the silylene leads mostly to enhanced π-bonding between nitrogen and carbon atoms, and does not contribute significantly to π-delocalization throughout the entire ring system.

**Natural Atomic Orbital and Natural Bonding Orbital Analyses.** Natural atomic orbital (NAO) method[26a,b] uses the one-electron density matrix of a molecular system to define the effective natural orbitals for atoms in a molecular environment. These orbitals can subsequently be subjected to natural population analysis (NPA) which yields values for atomic properties such as charge and atomic orbital occupancies. NAOs can also be used to describe the localized, Lewis-like, bonding pattern of electron pairs in a molecular system by forming an orthonormal set of localized natural bonding orbitals (NBOs) as linear combinations of several NAOs.[26c,d] Thus, NBO analysis provides a valence bond-type description of the system by giving a single most accurate possible Lewis-like depiction of the total electron density. Both NPA and NBO analyses have proven to be useful tools in the analysis of electronic structures of molecules[26d] and have also been used to analyze bonding in some of the systems discussed in the present study.[11f,g,15b,18a] Therefore, these methods provide the natural starting point for a comprehensive analysis of the electron density in **1-16**.

Table 3 summarizes the data obtained from NPA analysis of **1-16**. The calculated natural atomic charges for elements E reproduce the trends observed in Mulliken and APT charges reasonably well. However, the numeric values obtained from NPA analysis are in good agreement with Mulliken and APT charges only for structures in which the element E is from the second period. For all other systems, the NPA calculated charges are approximately 0.5 electrons more positive than the corresponding Mulliken and APT values. Such behavior is inherent to the NPA method, which tends to give an enhanced ionicity of bonds between elements with large differences in electronegativity.[27] This serves as a good illustration of how different methods partitioning the same electron density can come up with seemingly different values for atomic properties since there exists no unambiguous way to divide the total electron density between individual atoms in a molecule. One should therefore not put too much weight on numeric values, but instead look at the trends predicted with each method employed.

**Table 3.** Summary of Results from Natural Population Analysis of **1**-**16**[a]

| | $\delta E$ | $p_\pi E$ | $p_\pi N$ | $p_\pi C$ | $W_{EN}$ | $W_{NC}$ | $W_{CC}$ |
|---|---|---|---|---|---|---|---|
| ***1***; *E* = $B^-$ | –0.09 | 0.36 | 1.66 | 1.14 | 0.92 | 1.13 | 1.65 |
| ***2***; *E* = $Al^-$ | 0.39 | 0.26 | 1.72 | 1.13 | 0.51 | 1.18 | 1.64 |
| ***3***; *E* =$Ga^-$ | 0.35 | 0.27 | 1.71 | 1.13 | 0.53 | 1.19 | 1.63 |
| ***4***; *E* = $In^-$ | 0.34 | 0.32 | 1.69 | 1.12 | 0.51 | 1.21 | 1.60 |
| ***5***; *E* = *C* | 0.06 | 0.64 | 1.58 | 1.09 | 1.30 | 1.14 | 1.67 |
| ***6***; *E* = *Si* | 0.87 | 0.47 | 1.67 | 1.07 | 0.83 | 1.17 | 1.65 |
| ***7***; *E* = *Ge* | 0.90 | 0.49 | 1.66 | 1.08 | 0.79 | 1.19 | 1.62 |
| ***8***; *E* = *Sn* | 0.94 | 0.52 | 1.65 | 1.07 | 0.73 | 1.22 | 1.59 |
| ***9***; *E* = $N^+$ | 0.06 | 1.12 | 1.44 | 0.99 | 1.38 | 1.26 | 1.54 |
| ***10***; *E* = $P^+$ | 1.10 | 0.88 | 1.56 | 0.97 | 1.08 | 1.24 | 1.54 |
| ***11***; *E* = $As^+$ | 1.17 | 0.92 | 1.56 | 0.97 | 1.01 | 1.28 | 1.49 |
| ***12***; *E* = $Sb^+$ | 1.32 | 0.93 | 1.56 | 0.96 | 0.90 | 1.31 | 1.46 |
| ***13***; *E* = $O^{2+}$ | 0.08 | 1.68 | 1.37 | 0.78 | 1.12 | 1.57 | 1.21 |
| ***14***; *E* = $S^{2+}$ | 1.14 | 1.47 | 1.45 | 0.80 | 1.09 | 1.47 | 1.27 |
| ***15***; *E* = $Se^{2+}$ | 1.27 | 1.48 | 1.45 | 0.80 | 1.02 | 1.50 | 1.24 |
| ***16***; *E* = $Te^{2+}$ | 1.54 | 1.46 | 1.46 | 0.80 | 0.92 | 1.51 | 1.23 |

[a] Natural atomic charges ($\delta$), orbital populations ($p_\pi$), and Wiberg bond indices ($W$).

The occupancies of the formally empty natural atomic $p_\pi$ orbitals perpendicular to the ring plane in **1**-**16** are also listed in Table 3. The calculated values show that the occupancies follow a simple trend. When going from left to right across the periodic table, the $p_\pi$E occupancies increase while $p_\pi$N and $p_\pi$C occupancies decrease. The changes in $p_\pi$E and $p_\pi$N occupancies do not seem to correlate in any obvious way with the calculated NAO Wiberg bond indices $W$ which offer a general guide to bond orders (see Table 3). While this may be initially surprising, it becomes less so

if one compares the various $p_\pi$ occupancies with the shapes of π-symmetric MOs in Figure 1.[28] It is clearly visible that trends in $p_\pi$E and $p_\pi$N occupancies follow the changes in MOs discussed earlier. As a consequence, the observed increase in $p_\pi$E occupancy going from Group 13 to Group 16 systems leads to neither high NE bond orders nor to significantly enhanced π-delocalization throughout the five-membered ring as most of the electron density transferred from the formally doubly occupied $p_\pi$N orbitals becomes non-bonding, lone pair-type in character. If this effect is taken into account, the agreement between results from molecular orbital analysis, calculated $p_\pi$ orbital populations, and Wiberg bond indices is restored. This result also demonstrates that arguments relating $p_\pi$E occupancies with the degree of π-stabilization in the NEN fragment[11f,g,15b,16b,25] is not entirely justified for **1**-**16**.

It has been pointed out before that the relative contribution of the dicoordinate atom E to the $\pi_3$ MOs of **5**-**7** increases in the order C < Si < Ge.[16b] This was taken to indicate that the electronic structures of the heavier Group 14 imidazol-2-ylidene analogues include greater contribution from the chelated atom VB description shown in structure **I** for the Sn system. This naturally means that the NHC analogues **6**-**8** could serve as four electron donors alike the related bipyridyl systems.[29] Subsequent theoretical investigations contradicted the presented idea as smaller calculated NAO $p_\pi$E occupancies were obtained for the Si and Ge systems than for the parent carbon species.[15b] However, based on the above analysis, the $p_\pi$E NAO occupancies cannot be directly used to contradict the chelated atom model as they also mirror the changes in other MOs, in particular the $\pi_1$ orbital (see Figure 1).[30]

**Table 4.** Summary of Results from Natural Bond Orbital Analysis of **1**-**16**[a]

| | $\sigma_{EN}$<br>$\pi^{LP}{}_{N}$ | $\pi_{EN}$<br>$\pi^{*}{}_{EN}$ | $\sigma_{NC}$<br>$\pi_{NC}$ | $\sigma_{CC}$<br>$\pi_{CC}$ | $\sigma^{LP}{}_{E}$<br>$\pi^{LP}{}_{E}$ [$\pi^{*LP}{}_{E}$] | $\pi^{*}{}_{CC}$<br>$\pi^{*}{}_{NC}$ |
|---|---|---|---|---|---|---|
| ***1***; *E* = $B^{-}$ | *1.98 (20/80)*<br>*1.67* | *1.85 (10/90)*<br>*0.18 (90/10)* | *1.99 (60/40)* | *1.98 (50/50)*<br>*1.95 (50/50)* | *1.92* | *0.33 (50/50)* |
| ***2***; *E* = $Al^{-}$ | *1.97 ( 9/91)*<br>*1.72* | *1.84 ( 7/93)*<br>*0.14 (93/ 7)* | *1.99 (59/41)* | *1.98 (50/50)*<br>*1.94 (50/50)* | *1.97* | *0.33 (50/50)* |
| ***3***; *E* = $Ga^{-}$ | *1.97 (9/91)*<br>*1.71* | *1.82 ( 7/93)*<br>*0.15 (93/ 7)* | *1.99 (59/41)* | *1.98 (50/50)*<br>*1.93 (50/50)* | *1.98* | *0.34 (50/50)* |
| ***4***; *E* = $In^{-}$ | *1.97 ( 8/92)*<br>*1.69* | *1.69 (0/100)* | *1.99 (58/42)* | *1.98 (50/50)*<br>*1.91 (50/50)* | *1.99*<br>*[0.33]* | *0.35 (50/50)* |
| ***5***; *E* = *C* | *1.98 (34/66)*<br>*1.58* | *1.88 (20/80)*<br>*0.34 (80/20)* | *1.99 (61/39)* | *1.98 (50/50)*<br>*1.90 (50/50)* | *1.92* | *0.27 (50/50)* |
| ***6***; *E* = *Si* | *1.98 (16/84)*<br>*1.67* | *1.87 (13/87)*<br>*0.27 (87/13)* | *1.99 (60/39)* | *1.99 (50/50)*<br>*1.88 (50/50)* | *1.98* | *0.27 (50/50)* |
| ***7***; *E* = *Ge* | *1.97 (15/85)*<br>*1.66* | *1.87 (13/87)*<br>*0.29 (87/13)* | *1.99 (60/39)* | *1.99 (50/50)*<br>*1.87 (50/50)* | *1.98* | *0.29 (50/50)* |
| ***8***; *E* = *Sn* | *1.97 (13/87)*<br>*1.65* | *1.86 (13/87)*<br>*0.32 (87/13)* | *1.99 (59/41)* | *1.99 (50/50)*<br>*1.84 (50/50)* | *1.99* | *0.30 (50/50)* |
| ***9***; *E* = $N^{+}$ | *1.99 (46/54)*<br>*1.49* | *1.91 (37/63)*<br>*0.65 (63/37)* | *1.99 (62/38)* | *1.98 (50/50)*<br>*1.73 (50/50)* | *1.94* | *0.25 (50/50)* |
| ***10***; *E* = $P^{+}$ | *1.98 (25/75)*<br>*1.56* | *1.90 (25/75)*<br>*0.55 (75/25)* | *1.99 (62/38)* | *1.99 (50/50)*<br>*1.72 (50/50)* | *1.98* | *0.24 (50/50)* |
| ***11***; *E* = $As^{+}$ | *1.98 (22/78)*<br>*1.56* | *1.90 (26/74)*<br>*0.59 (78/22)* | *1.99 (61/39)* | *1.99 (50/50)*<br>*1.68 (50/50)* | *1.99* | *0.27 (50/50)* |
| ***12***; *E* = $Sb^{+}$ | *1.98 (18/82)* | | *1.99 (60/40)*<br>*1.91 (73/27)* | *1.99 (50/50)* | *1.99*<br>*0.93* | *0.61 (27/73)* |
| ***13***; *E* = $O^{2+}$ | *1.99 (56/44)* | | *1.99 (62/38)*<br>*1.91 (68/32)* | *1.98 (50/50)* | *1.97*<br>*1.68* | *0.24 (32/68)* |
| ***14***; *E* = $S^{2+}$ | *1.98 (34/66)* | | *1.99 (62/38)*<br>*1.91 (70/30)* | *1.98 (50/50)* | *1.99*<br>*1.48* | *0.34 (29/71)* |
| ***15***; *E* = $Se^{2+}$ | *1.98 (30/70)* | | *1.99 (62/38)*<br>*1.92 (71/29)* | *1.98 (50/50)* | *1.99*<br>*1.49* | *0.33 (29/71)* |
| ***16***; *E* = $Te^{2+}$ | *1.98 (23/77)* | | *1.99 (61/39)*<br>*1.93 (70/30)* | *1.99 (50/50)* | *1.99*<br>*1.47* | *0.33 (30/70)* |

[a] NBO populations and their percentage contributions (in parenthesis).

The electronic structures of **1**-**16** can also be analyzed in terms of NBOs (*i.e.* multi-centered orbitals) which offer a more accessible approach to bonding in main group carbene analogues. Data from such calculations are presented in numeric form in Table 4 which includes NBO populations and their individual contributions; graphical depiction of the data is shown in Figure 2. According to the NBO analysis, structures **1**-**3** and **5**-**11** all contain a three-center-four-electron π-bond in their

NEN moiety as well as one CC double bond with a notable delocalization contribution (average population in $\pi^*_{CC}$ NBO is 0.30). The π-electrons in the three-center-four-electron bond are distributed among three NBOs, $\pi_{EN}$, $\pi^{LP}{}_N$, and $\pi^*{}_{EN}$, which indicates that bonding within the NEN fragment can be conveniently described with two resonance structures of the type $N{=}\ddot{E}{-}\ddot{N} \leftrightarrow \ddot{N}{-}\ddot{E}{=}N$. Despite such uniform feature in their electron density, the properties of individual NBOs also reveal important differences for systems **1**-**11**. As seen from Table 4, the NE bonds are ionic in all Group 13 carbene analogues, whereas bonding in all Group 14, and especially in Group 15 systems, is more covalent in nature. Hence, though the single best Lewis structure for **1**-**3** formally contains an EN double bond, the proper description of electron density in Group 13 carbene analogues requires the inclusion of additional, more ionic, resonance structures.[31] The electronic structures of the heavier Group 13 anions **2**-**4** could also be described by a chelated atom model which would properly describe the polarization present in both $\sigma_{EN}$ and $\pi_{EN}$ NBOs. However, the chemical behavior displayed by the compounds is not fully consistent with this model (see below).

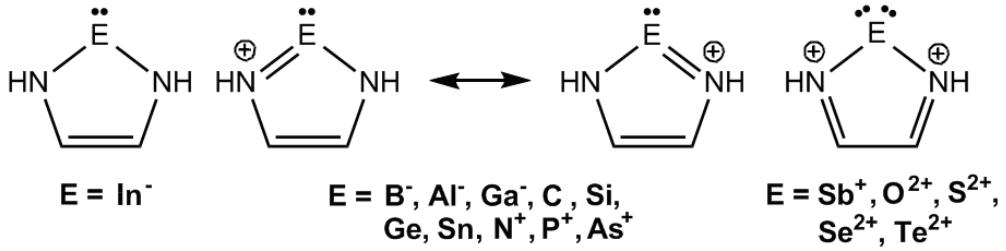


**Figure 2.** Single best Lewis depictions of the total electron density in **1**-**16** based on results from NBO analysis.

Alike to the trend observed for the Group 13 systems, the importance of the doubly EN bonded resonance structure in describing the electron density in **6**-**8** is diminished due to greater bond polarization. An increasing amount of delocalizing, non-Lewis, interactions are also observed when comparing Group 14 and 15 carbene analogues to Group 13 systems as indicated by the trends in $\pi^*_{EN}$ and $\pi_{CC}$ populations. In particular, the deviation of the $\pi_{CC}$ population from the ideal value 2, together with the high non-Lewis occupancy of the $\pi^*{}_{EN}$ NBO (around 0.60 electrons)

indicate that the electronic structures of **9**-**11** have a significant contribution from a resonance structure containing two CN double bonds. Hence, the cationic Group 15 analogues of imidazol-2-ylidene are expected to display stronger electron delocalization than that readily inferable from the two resonance structures shown in Figure 2.

The transformation in the electronic structures of **1**-**16** observed earlier in the MO analysis becomes evident when results for the stibenium cation **12** and the chalcogenium dications **13**-**16** are examined. In these systems, both the $\pi_{EN}$ and $\pi_{CC}$ NBOs are formally empty as π-electron population is distributed between the two NC bonds and the p-type lone pair orbital centered on the element E (see Table 4). Hence, the element E bears two distinct lone pairs of electrons and the electronic structure of the NCCN moiety resembles that found for a free *cis*-DAB ligand; the best single Lewis description of the electronic structures of **12**-**16** is shown in Figure 2. It should however, be emphasized that the above description is again an oversimplification of the true electron distribution in **12**-**16** as electron population in the $\pi^{LP}_{E}$ and $\pi^{*}_{NC}$ NBOs remains less than 2 and much higher than zero, respectively.

Taken as a whole, the results of NBO analysis corroborate the picture gathered from MO analysis: (i) The electronic structures of **1**-**16** run the gamut from C=C localized to C=N localized *via* more delocalized, intermediate systems. (ii) Cyclic electron delocalization seems to play a prominent role only in the parent carbon species, the lighter Group 15 cations, and (to a lesser extent) in Group 16 dications. The electronic distribution found for **12**-**16** gives a new perspective to the discussion that has been presented in the context of Group 14 systems **6**-**8**.[11f,15b,16b] Although the current analyses show that the chelated atom model used to describe bonding in the Group 16 systems has a non-dominant role in the VB wave function of any of the Group 14 analogues, the results prove the earlier predictions that the importance of this effect increases as the atomic number of the dicoordinate main group centre increases.[16b] Hence, the chelate-type structure **I** represents a somewhat exaggerated picture of the true electronic polarization in **6**-**8** and even the heavier

germylene and stannylene imidazol-2-ylidene analogues can be considered to contain the Group 14 element in a formal +II oxidation state.[15b,11f,16b,32,33] This might, however, not be the case for all main group carbenes: the four coordinate structures observed for the metal complexes of Group 14-bipyridyl systems[29] are most likely influenced by the electron delocalization in the bipyridyl moiety which leads to different electronic configuration around the Group 14 element as compared to **6-8**.[34] It can be envisaged that a similar effect could possibly be induced in systems **6-8** through an appropriate substitution pattern. In addition, even though the free carbene analogues **6-8** can be considered to contain the Group 14 element in a formal +II oxidation state, the chelated atom model might nevertheless have an influence to their reactivity: it has been shown that, unlike NHCs, the *N*-heterocyclic silylenes can act as a bridging ligand to Pd(0), giving rise to a dinuclear complex with four-coordinate Group 14 centers.[35]

**Electron Localization Function.** In the previous sections, the electronic structures of **1-16** were analyzed using two methods based on orbitals, either Kohn-Sham orbitals or NAOs. Although these methods lead to similar conclusions at qualitative and quantitative levels, some criticism is perhaps warranted as both approaches use mathematical constructs whose physical meaning is anything but self-explanatory not only to describe the electron density, but also in the actual analysis.[36] To ensure that the conclusions drawn remain independent of the chosen approach, the electron densities in **1-16** should also be analyzed with an approach that is essentially orbital-free. Two of the most popular methods which fill this criterion are the atoms-in-molecules (AIM) theory[37] and the analysis of the electron localization function (ELF).[38] Common to both methods is that they use topological analysis to examine a continuous and differentiable scalar field in the three-dimensional space, electron density in the former and the electron localization function in the latter case. In this study, the ELF approach was adopted.

The electron localization function is an orbital independent description of relative electron localization, defined as the ratio of excess kinetic energy density due to the Pauli exclusion

principle and Thomas-Fermi kinetic energy density.[38] ELF describes the interaction between same-spin electrons. In regions of space where Pauli repulsion is weak ELF attains values close to unity, whereas the probability of finding the same-spin electrons close together is high the numerical value of ELF approaches zero. Since ELF is a scalar function, topological analysis of its gradient field can be used to obtain further, chemically relevant, information. The molecular space is partitioned in basins of attractors which have a one-to-one correspondence with concepts from Lewis' valence theory (*i.e.* core-electrons, bonds, and lone pairs). Qualitative, graphical representations of bonding are obtained by plotting isosurfaces of ELF which delimit volumes within which the Pauli repulsion is rather weak. The partition of the molecular space also enables basin-related properties such as population and variance to be calculated with quantitative accuracy by integrating a given density of the property over the volume of the basins.

The electronic structures of **1**-**16** were subjected to ELF analysis and a summary of results is shown in Table 5. Plots of ELF isosurfaces are pictured in Figure 3. Changes in ELF basins' shapes and populations echo results from orbital-based analyses extremely well. For example, ELF analysis locates a typical C=C double bond in each of the structures **1**-**8** and assigns the lone pair electrons formally residing on the nitrogen atoms to two larger disynaptic *V*(EN) valence basins (*cf.* results from NBO analysis). The relative fluctuations (the ratio of variance and basin population) for *V*(NC) and *V*(CC) basins in **1**-**8** indicate that bonding electrons within the NCCN fragment are delocalized ($\lambda > 0.5$).

Starting from the nitrogen NHC analogue **9**, a transformation in the structure of the ELF emerges. The two *V*(CC) basins merge into a superbasin, whose population decreases roughly by 0.4 as electrons are transferred mainly to the *V*(NC) bond basins. A decrease in electron population in *V*(EN) bond basins is also observed together with a concomitant increase in the *V*(E) lone pair basin population. As noted earlier, the stibenium cation is the first one in the series to display both σ- and π-symmetric lone pair NBOs on element E. In the ELF, an analogous separation of the lone

pair basin to two protruding lobes directed diagonally above and below the molecular plane occurs which corresponds well with the classical "rabbit ear" distribution of electron pairs. This feature is also inherent to the electronic structures of all chalcogen dications **13-16** for which the transfer of electron population from CC and EN bonds to the two *V*(NC) bond basins is found to be even more complete.[39] A side view plot of ELF for Period 4 systems in Figure 4 better illustrates the above changes in the *V*(E) basin.

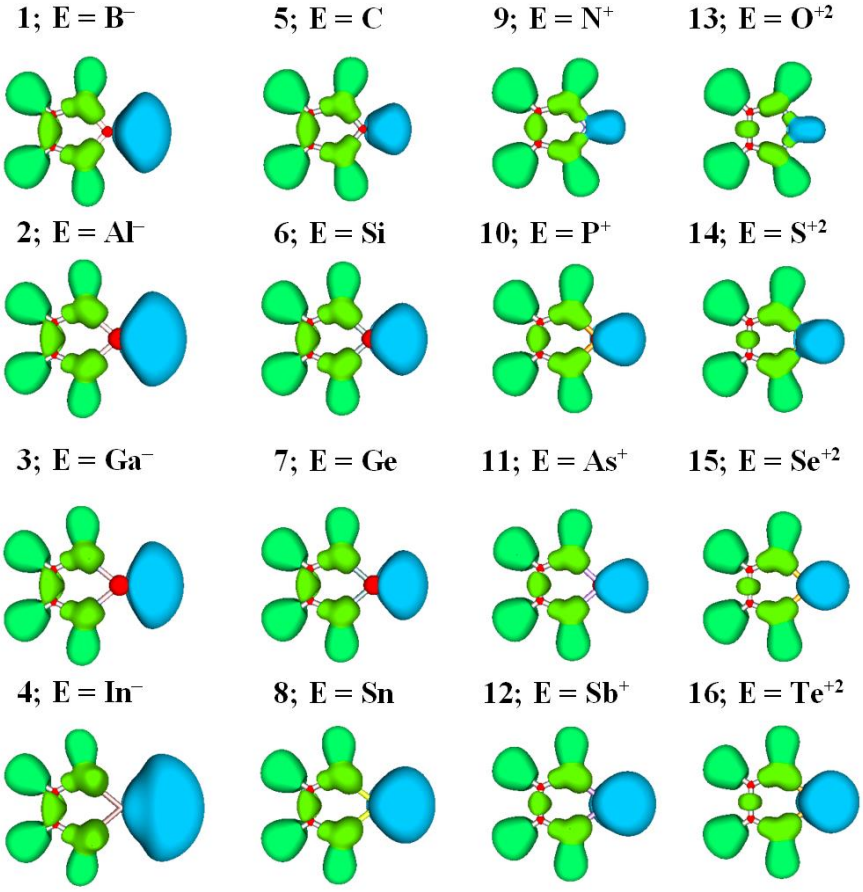


**Figure 3.** ELF isosurface plots ($\eta$ = 0.7) of **1-16**; basin color code: core = red, lone pair = blue, bonding = green.

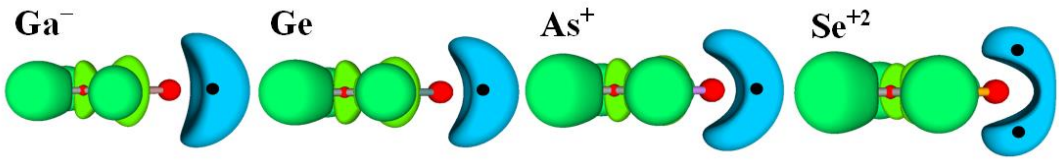


**Figure 4.** Side view of ELF isosurface plots ($\eta$ = 0.7) of **3**, **7**, **11**, and **15**. Basin color code: core = red, lone pair = blue, bonding = green; black spot denotes lone pair basin attractors.

**Table 5.** Summary of Results from Electron Localization Function Analysis of **1**-**16**[a]

| | *V(E)* | *V(EN)* | *V(NC)* | *V(CC)* |
|---|---|---|---|---|
| | $\overline{N}$ *(λ)* | $\overline{N}$ *(λ)* | $\overline{N}$ *(λ)* | $\overline{N}$ *(λ)* |
| ***1**; E = $B^-$* | *2.17 (0.31)* | *3.66 (0.43)* | *1.91 (0.55)* | *2 × 1.83 (0.57)* |
| ***2**; E = $Al^-$* | *2.16 (0.30)* | *3.76 (0.40)* | *1.90 (0.56)* | *2 × 1.82 (0.57)* |
| ***3**; E =$Ga^-$* | *2.42 (0.45)* | *2 × 1.86 (0.57)* | *1.92 (0.55)* | *2 × 1.81 (0.57)* |
| ***4**; E = $In^-$* | *2.33 (0.51)* | *2 × 1.84 (0.57)* | *1.94 (0.55)* | *2 × 1.81 (0.57)* |
| ***5**; E = C* | *2.47 (0.36)* | *3.43 (0.46)* | *1.99 (0.54)* | *2 × 1.76 (0.57)* |
| ***6**; E = Si* | *2.45 (0.36)* | *3.60 (0.43)* | *1.99 (0.55)* | *2 × 1.75 (0.57)* |
| ***7**; E = Ge* | *2.75 (0.48)* | *3.52 (0.45)* | *1.99 (0.55)* | *2 × 1.74 (0.57)* |
| ***8**; E = Sn* | *2.60 (0.54)* | *2 × 1.77 (0.58)* | *1.99 (0.55)* | *2 × 1.72 (0.58)* |
| ***9**; E = $N^+$* | *3.09 (0.38)* | *1.90 (0.56)* | *3.24 (0.48)* | *3.15 (0.45)* |
| ***10**; E = $P^+$* | *2.93 (0.39)* | *3.17 (0.47)* | *2.17 (0.53)* | *3.19 (0.45)* |
| ***11**; E = $As^+$* | *3.33 (0.49)* | *3.12 (0.49)* | *2.22 (0.52)* | *3.13 (0.45)* |
| ***12**; E = $Sb^+$* | *2 × 1.58 (0.65)* | *3.19 (0.48)* | *2.20 (0.53)* | *3.10 (0.45)* |
| ***13**; E = $O^{2+}$* | *2 × 2.25 (0.49)* | *1.26 (0.65)* | *2 × 1.74 (0.58)* | *2.44 (0.48)* |
| ***14**; E = $S^{2+}$* | *2 × 1.94 (0.51)* | *1.89 (0.56)* | *3.19 (0.47)* | *2.59 (0.47)* |
| ***15**; E = $Se^{2+}$* | *2 × 2.10 (0.56)* | *2.07 (0.56)* | *3.07 (0.47)* | *2.57 (0.47)* |
| ***16**; E = $Te^{2+}$* | *2 × 1.96 (0.58)* | *2.51 (0.53)* | *2.73 (0.49)* | *2.55 (0.47)* |

[a] Average basin populations $\overline{N}$ and their relative fluctuations $\lambda$ (in parenthesis).

**Aromatic Delocalization.** The concept of aromaticity is of central importance in organic chemistry. Despite its essential status, aromaticity is a multidimensional characteristic, which is extremely difficult to define quantitatively and various criteria based on geometric, energetic, magnetic, and electronic properties have been employed to delineate aromaticity in different chemical systems.[40] Our results from calculations probing the energetic and magnetic properties of

**1-16**, and are discussed in the context of aromatic stabilization. This topic has already been touched in MO, NBO, and ELF analyses, so the primary aim of the current discussion is to broaden its scope by comparing quantitative measures of electron delocalization in **1-16** as given by the different computational approaches. Some of the applied methods have been used to analyze the electronic structures of Group 14 and 15 systems **5-7** and **8-9** in the past.[11d,g,h,15,17b] In these cases, our results agree with the published data. However, to facilitate comparison of the previously unanalyzed systems to the ones for which computational data exists, the results reported below are listed for all systems **1-16**.

Table 6 lists the energies calculated for isodesmic hydrogenation reactions (1) and (2) for **1-12**, from which the aromatic stabilization energies (ASEs) are readily obtained as their difference. Calculated ASEs for **1-12** are also included in Table 6. We note that the numbers given in Table 6 might differ from the values reported in the literature as there is no single definition of aromatic stabilization energy and the results are always dependent on the choice of the model system. As seen, the ASEs calculated from the simple hydrogenation reactions are smallest for Group 13 systems and largest for Group 15 NHC analogues. Within each group, the largest ASE is found for systems incorporating the lightest elements E, which is in good agreement with conclusions drawn from MO and NBO analyses in that electron delocalization throughout the five-membered ring is most effective for Period 2 systems. However, the trend in ASEs is not solely decreasing upon descending the group. The energies calculated for Period 4 and 5 systems are generally larger than those calculated for Period 3 species. In fact, indium and tin NHC analogues are found to contain almost as much ASE as their lighter boron and carbon homologues! This effect naturally mirrors the gradual changes taking place in the electronic structure of the NCCN moiety and therefore, cannot be used as a direct indication of greater electron delocalization throughout the five-membered ring in the heavier element homologues as compared to the Period 2 systems.

The thermodynamic stability and π-stabilization in **1-12** can also be evaluated by calculating hydrogenation energies for reaction (3) and comparing these values with energies calculated for similar reaction between unsubstituted systems (4).[41] Such an approach complements the ASE calculations as the energy difference (3) – (4) is not as sensitive to changes in the electronic structure of the NCCN moiety, but represents relative aromatic stabilization due to electron delocalization within the NEN fragment and also throughout the entire five-membered ring. The calculated numbers are, however, not totally comparable between different groups as values for Group 13 and 15 species can be selectively influenced by charge delocalization which is not a pure π-effect *per se*.

**Table 6.** Energies for Hydrogenation Reactions (1), (2), (3), and (4) [kJ mol$^{-1}$].

| | *(1)* | *(2)* | *(3)* | *(4)* | *(1) – (2)* | *(3) – (4)* |
|---|---|---|---|---|---|---|
| ***1**; E = B*$^-$ | *–76* | *–118* | *–415* | *–184* | *42* | *230* |
| ***2**; E = Al*$^-$ | *–65* | *–94* | *–212* | *–11* | *29* | *201* |
| ***3**; E =Ga*$^-$ | *–62* | *–96* | *–180* | *–51* | *34* | *129* |
| ***4**; E = In*$^-$ | *–55* | *–105* | *–104* | *–21* | *50* | *84* |
| ***5**; E = C* | *–84* | *–151* | *–579* | *–102* | *67* | *477* |
| ***6**; E = Si* | *–76* | *–125* | *–260* | *–50* | *50* | *210* |
| ***7**; E = Ge* | *–63* | *–125* | *–196* | *35* | *62* | *231* |
| ***8**; E = Sn* | *–55* | *–117* | *–106* | *102* | *62* | *208* |
| ***9**; E = N*$^+$ | *–66* | *–188* | *–846* | *97* | *122* | *943* |
| ***10**; E = P*$^+$ | *–70* | *–168* | *–367* | *67* | *98* | *434* |
| ***11**; E = As*$^+$ | *–48* | *–163* | *–267* | *154* | *115* | *421* |
| ***12**; E = Sb*$^+$ | *–37* | *–145* | *–137* | *211* | *108* | *348* |

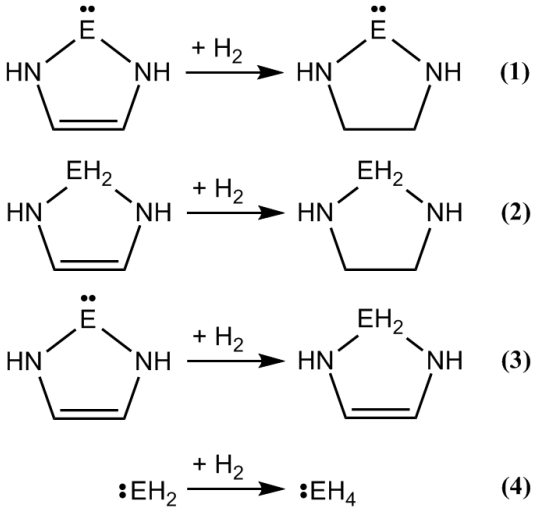


The calculated delocalization energies (see Table 6) show that all systems **1-12** are significantly stabilized compared to the unsubstituted species :$EH_2$. The energy difference (3) − (4) is exceptionally large for Period 2 systems (almost 950 kJ $mol^{-1}$ for the nitrenium species) and decreases significantly when moving to Period 3 systems and below due to the gradual loss of π-bonding within the NEN fragment. It is interesting to note that the calculated delocalization energy is essentially constant for Si, Ge, and Sn imidazol-2-ylidene analogues (approximately 220 kJ $mol^{-1}$). The delocalization energies calculated for the heavier Group 15 carbene analogues **10** and **11** are very close to the value obtained for the parent carbon system, indicating equal level of aromatic delocalization in these structures. This result is in good agreement with data from orbital and electron density analyses, but disagrees with the calculated ASEs reported above which showed greater energetic stabilization in **9-12** as compared to **5**. The different outcome of the two energetic measures of aromaticity results from the fact that the chosen hydrogenation reactions do not treat the features in the electronic structures of **1-12** in a uniform manner (see above). This problem is inherent to all energetic analyses used to quantify aromatic character.

Neither one of the above energetic approaches could be applied to study the chalcogen systems **13-16** because addition of hydrogen atoms to the Group 16 elements immediately lead to ring opening. For this reason, electron delocalization in the chalcogen analogues of imidazol-2-

ylidene was analyzed using the energetic analysis implemented in the NBO approach. The role of electronic delocalization can be quantitatively assessed with this method by choosing a reference Lewis-type electronic structure to describe bonding, carrying out the NBO analysis and then deleting all non-Lewis contributions present in the system. The resulting natural Lewis structure is perfectly localized with all Lewis-type NBOs doubly occupied and all other NBOs empty. The energy of such a hypothetical structure can be calculated and compared to the energy of an unaltered system from which the stabilizing, delocalization energy is readily obtained.

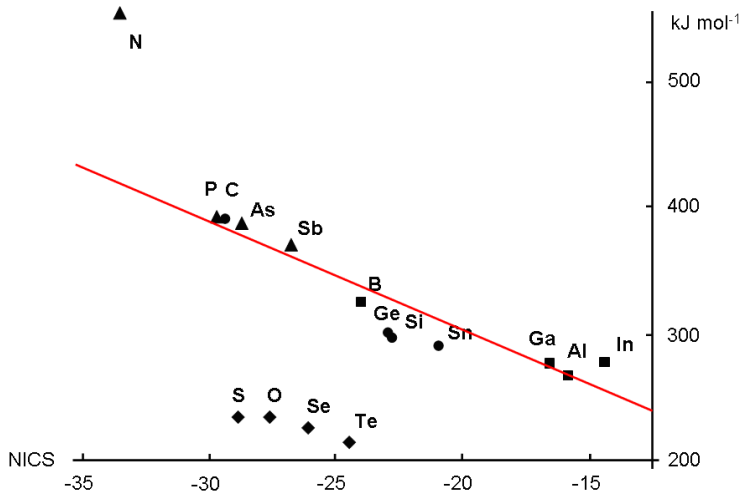


**Figure 5.** NBO delocalization energies (*y*-axis) plotted against the calculated NICS values (*x*-axis).

NBO calculations show that electron delocalization in **13-16** increases the stability of these systems by about 220 kJ $mol^{-1}$ when their electronic structures are compared to Lewis structures with two perfectly localized C=N double bonds. If the electronic structures of cations **13-16** are compared to Lewis structures in which the diazabutadiene ligand has an N–C=C–N bonding arrangement, the energy difference increases to approx. 600 kJ $mol^{-1}$. For comparison, the NBO derived delocalization energy in the parent carbon system **5** is 390 kJ $mol^{-1}$ and 690 kJ $mol^{-1}$, respectively, compared to the perfectly C=C and C=N double bonded alternatives. This once again confirms the fact that the C=N doubly bonded Lewis structure is a closer approximation of the true electron density distribution in **13-16** and that delocalization of the four π-electrons in the two CN

double bonds makes a fairly strong additional stabilizing contribution. NBO delocalization energies were also calculated for other analogues of imidazol-2-ylidene **1**-**12**. As the results confirm all of the conclusions drawn above, an in-depth discussion is not warranted.[42]

Another technique for the evaluation of relative aromatic stabilization, which is able to treat all systems **1**-**16** on an equal footing, is the calculation of nucleus independent chemical shifts (NICSs). NICS is a method based on the theoretical chemical shielding tensor (sign reversed) for a ghost atom residing at, or slightly above the center of an aromatic ring system.[43] Significantly negative NICS values inside rings and cage structures indicate the presence of strong diatropic ring currents and denote aromaticity, whereas positive values indicate opposite, anti-aromatic behavior. The performance of different NICS-based indices as generally applicable criteria to characterize aromaticity has been reviewed recently.[43b,c] The slightly different NICS indices all perform reasonable well for a variety of aromatic ring systems and show good agreement with calculated aromatic stabilization energies. In this study, the NICS values were calculated 1 Å above the molecular plane and only the zz component of the magnetic shielding tensor is used in the analysis *i.e.* $NICS(1)_{zz}$.[43c]

The calculated NICS values for **1**-**16** are plotted in Figure 5 against delocalization energies obtained from NBO energy analysis; ASE values were not used in the plot as they could not be determined for the chalcogen systems **12**-**16**. The correlation between the two measures of aromaticity is not very good if all 16 compounds are considered. The most obvious outlier is the nitrenium cation **9** whose NBO derived delocalization energy indicates much greater level of aromaticity than that inferred from its $NICS(1)_{zz}$ value. This disagreement arises from the extremely strong π-bonding interactions present in the NNN fragment which contribute significantly to its energy, but do not enhance cyclic electron delocalization, and therefore the diatropic ring current in **9** in similar proportion. In addition, even though correlation within the Group 16 systems is fairly linear, the points for these species in Figure 5 lie well below the correlation line determined using

data for the remaining eleven species ($r$ = 0.94). The observed discrepancy originates from the differences in the electronic structures of **13**-**16** as compared to **1**-**12**. Since different reference Lewis structures were used in the NBO analysis, the calculated energies are unfit for direct comparison. Nevertheless, the correlation between the NBO delocalization energies and the calculated $NICS(1)_{zz}$ values is very good if the two sets of compounds are treated independently. The values shown in Figure 5 can also be compared with the $NICS(1)_{zz}$ value calculated for cyclopentadienide (–33.9 ppm), which indicates that electron delocalization is significant in all but the heaviest Group 13 and 14 carbene analogues **2**-**4** and **6**-**8**.

Because the different methods used to delineate electron delocalization in **1**-**16** give slightly different results, it is impossible to put these systems in any exact order with respect to aromaticity. Some general conclusions can, however, be drawn. First, all methods indicate that π-electron delocalization contributes the least to the stabilization of Group 13 analogues of imidazol-2-ylidene. Second, the nitrenium cation **9** seems to benefit the most from aromatic stabilization based on both energetic and magnetic criteria employed. The rest of Group 15 cations are more or less on par with the parent carbon system, the former benefiting more from aromatic stabilization within the NCCN fragment and the latter from electron delocalization throughout the entire five-membered ring. Though the extent of electron delocalization in **9** and **10** has already been reported in the literature,[11d,g,h,17b] it is interesting to note that the analyses gave similar results also for the arsenium cation **11**: both the calculated stabilization energies and $NICS(1)_{zz}$ values indicate nearly equal level of aromaticity for the three Group 15 cations. Third, the chalcogen NHC analogues **13**-**16** display ambivalent behavior in the two analyses employed: the presence of two fairly localized CN double bonds leads to small NBO delocalization energies, but the calculated NICS values verify the existence of diatropic ring currents which are almost as strong as those calculated for the parent NHC.

**σ-Donor Character.** As already mentioned in the introduction, NHCs are excellent σ-donor ligands which have found multitude of applications in chemical reactions. In this respect, it is interesting to compare the key features in the electronic structures of different main group carbene analogues to the parent carbon species and to determine to which extent the electron donor characteristics are mirrored in its isovalent main group analogues.

The presence of two lone pairs in the cations **12**-**16** became apparent in both NBO and ELF function analyses (see above). Hence, it is expected that these systems do not display similar bonding properties as observed for NHCs. This result rationalizes some earlier computational findings for the coordination compounds of Group 15 carbene analogues.[17d] While studying the properties of cations **10**-**12** as ligands in transition metal complexes, it was found that the stibenium ion coordinates to $Co(CO)_3$ with a pyramidal coordination sphere around the pnictogen atom, whereas similar complexes with the phosphenium and arsenium ligands **10** and **11** exhibit planar coordination modes. It is evident that the results are a direct manifestation of the different electronic structure of the stibenium cation as compared to the phosphenium and arsenium systems: the planar coordination mode is not observed for **12** due to the presence of two lone pairs, one above and one below the molecular plane.

Considering systems **1**-**11**, the frontier MO theory predicts that molecules which have their electron donating orbitals high in energy will be good electron donors and vice versa. Unfortunately a direct comparison of the calculated orbital energies for carbene analogues with elements E from different groups is impossible due to the lack of uniform zero-energy level for all systems. Some general remarks can, however, be made. First, the change in formal charge at the central element changes the reactivities of the carbene analogues, in that they range from being nucleophilic (Group 13 and 14) to amphiphilic (Group 15). Second, the relative ordering of frontier orbitals within different members of each group show that the energy of the σ-donating MO is lowered when going

down the group (see Supporting Information), indicating decreased nucleophilicity for systems in which E is a heavier p-block element ($n \geq 4$).

Though the boryl anion **1** is both computationally[18a] and experimentally[11a] a strong nucleophile, it has been proposed that the valence electron distribution in all other Group 13 carbene analogues could facilitate also electrophilic behavior:[44d] the electronic structures of all heavier Group 13 systems have previously been described with a donor-acceptor formulation **II** which contains a formally positively charged Group 13 center.[18a] In addition, an atoms-in-molecules analysis conduced for anions **1**-**4** indicated that the non-bonding σ-symmetric lone pair (orbital) becomes diminished in all heavier Group 13 carbene analogues as electron density is transferred from element E to the more electronegative nitrogen centers. However, results from MO, NBO, and ELF analyses presented above do not fully corroborate this description as they show significantly less than one unit of charge for element E and identify a chemically active lone pair of electrons around the divalent main group center in all Group 13 systems. Furthermore, both NBO and ELF analyses actually indicate that the lone pair orbital/basin populations increase as the element E becomes heavier (see Tables 4 and 5).

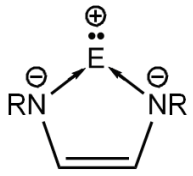


**II**
**E = Al, Ga, In**

While it is certainly true that the σ-symmetric orbital bearing the lone pair of electrons in **1**-**4** gains more s-character as the element E becomes heavier, it does not lead to significantly diminished nucleophilicity and Lewis base properties as readily inferable from previous analyses. The Laplacian of the electron density in **1**-**4** naturally mirrors the change in orbital characteristics by becoming more diffuse around the Group 13 nuclei when going down the group, but in all cases it still retains a [3,–3] critical point corresponding to the lone pair of electrons. This was verified by

performing an atoms-in-molecules analysis for **1**-**4** which located the sought-after maxima at expected locations. The Lewis base properties of the known anionic gallium carbene analogues towards various metals has also been recently demonstrated experimentally[44] which clearly shows that the previous assumption of a chemically more inert electron pair in heavier homologues of **1** is not entirely warranted.

**π-Acceptor Character.** NHCs have long been considered as pure σ-donors, and only very weak π-acceptors. Recent computational and experimental investigations have, however, questioned the validity of this generalization:[45] studies on various NHC systems have shown that π orbital interactions between ligands and transition metals are generally non-negligible and can in some specific cases represent almost one third of the total orbital interaction energy. It is thus evident that the capabilities of NHCs as π-acceptors are far greater than previously realized.

Both experimental and computational analyses of the π-acceptor nature of different main group carbene analogues have been reported for **3**[44a,e] as well as for cations **10**-**12**[17d,46]; theoretical analyses have been reported for **5**-**7**.[45a,47] Spectroscopic and structural studies have shown the presence of considerable metal-phosphorous double bond character in coordination complexes of **10** and short metal-pnictogen bonds with π-bonding contributions have been observed for analogous compounds with arsenic and antimony. Though the tendency of the heavier pnictogen monocations **10**-**12** to participate in metal-to-ligand backbonding interactions has been noted in the literature,[17d,46] it has not been rationalized why this effect contrasts with the known electrophilicities of individual systems. In particular, the CC-saturated analogue of **10** displays greater electrophilicity but lesser π-acidity than the unsaturated phosphenium carbene analogue.

The π-acceptor strength of NHCs is related to the energetic accessibility of the vacant molecular orbital with appropriate symmetry characteristics. According to frontier MO theory, the lower in energy this orbital is, the better an electron acceptor the system becomes. For the parent carbon system **5**, the vacant π orbital with a significant contribution from the carbene carbon is not

the LUMO but the LUMO+2, which resides 7.5 eV above the HOMO. The large orbital energy gap between the HOMO and the vacant π-acceptor orbital in the parent NHC is a direct manifestation of the properties of the occupied π orbitals discussed earlier. Since the carbon $p_\pi$ orbital makes a significant stabilizing contribution to both $\pi_1$ and $\pi_3$ bonding MOs, its contribution to the anti-bonding orbitals becomes destabilizing, increasing the energy of the vacant π-acceptor orbital. The smallest orbital energy gaps are calculated for the Group 13 carbene analogues, only 3.3 eV for the indium species **4**, which, however, does not lead directly to superior electron accepting abilities due to the presence of negative charge in **1**-**4**; the poor π-acceptor strength of the gallium system **3** has been reported recently.[44a] The orbital energy gap is also reasonably small for all Group 15 carbene analogues (between 4.0 and 5.2 eV) which, along with their overall positive charge, readily explains the experimental observations of their good backbonding capabilities.[17c,d,46]

Because π-acidity in **10**-**12** is only indirectly related to their positive charge distribution, the earlier observations regarding the lack of correlation between electrophilicity and π-acceptor strength in these systems is understandable.[17d] Though the CC-saturated analogue of **10** contains a charge distribution which localizes more positive charge on the divalent Group 15 element (calculated Mulliken charge is 0.65), it also increases the energy gap between the HOMO and the vacant π-acceptor orbital by 0.1 eV as compared to **10**. Analogous frontier MO theory arguments are also able to explain why charge decomposition analyses conducted for **5**-**7** yielded smaller donation/backdonation ratios for systems with heavier Group 14 elements than for the parent carbon species.[45a,47] However, it must be pointed out that electrostatic effects and the relative orbital energy differences between the ligand and the metal fragment are both very important factors which affect the overall nature of the metal-ligand bond. Hence, the strength of a particular carbene analogue system as a π-acceptor (and also as a σ-donor) is dependent on the metal to which it binds, as well as on the overall charge of the formed complex. Although the nature of the interaction should be determined separately for each particular combination, the above results, together with some

recently published analyses for the parent carbene **5**,[45c] allow some general guidelines to be given. It can be expected that the π-acceptor capabilities of **1-16** will increase slightly when going down the group or from left to right in the periodic table. Interactions of the different ligands with $d^{10}$ metals should also have larger metal-to-ligand backdonation contributions than with metals having either a partially or a fully unoccupied d-shell.

**Conclusion**

The electronic structures of 15 main group carbene analogues **1**-**4** and **6**-**16** were analyzed with various quantum chemical methods and compared to the parent system **5**. The current study represents the first systematic attempt to determine to which extent the different p-block *N*-heterocyclic carbene analogues mimic the electronic structure and properties of imidzol-2-ylidene. The most important conclusions drawn from the results are as follows:

1. Though all systems **1-16** are formally isovalent, the theoretical analyses indicate that the electronic structure of the stibenium ion as well as that of all chalcogenium dications differs from what would be expected for true carbene analogues. In particular, the cations **12-16** contain not one, but two lone pairs of electrons around the divalent element, directed diagonally above and below the molecular plane. Hence, systems **12-16** can be expected to display chemical reactivity atypical for **1-11**, which were all found to contain only one chemically active lone pair of electrons in a σ-symmetric orbital.

2. Different theoretical analysis methods uniformly showed that the electronic structures of **1-16** run the gamut from C=C localized (Group 13 carbene analogues) to C=N localized (Group 16 carbene analogues) via intermediate, more delocalized systems. Simple Lewis-type descriptions of the electronic structures of **1-16** were sketched out based on the results of NBO analyses. For the heavier Group 13 carbene analogues, the resonance structure in which a DAB ligand chelates a Group 13 anion becomes dominating, whereas the electronic structures of the heavier Group 16

carbene analogues as well as the stibenium cation **12** are best approximated with models in which the pnictogen/chalcogen element holds two electron pairs. The electronic structures of the Group 14 and 15 systems fall in between these two extremes and can be considered to contain the divalent element in either +II or +III formal oxidation state, respectively (oxidation state 0 for the nitrenium species **9**).

3. The aromatic character of **1-16** was analyzed using theoretical methods based on both energetic and magnetic properties. Results from different analyses were in good mutual agreement and indicated that all main group carbene analogues display some level of aromaticity. The heavier Group 13 systems benefit the least from aromatic stabilization whereas the lighter Group 15 systems are on par with the parent carbene **5**. The nitrenium ion was found to display diatropic ring currents as strong as those calculated for cyclopentadienide, a true 6π-electron aromatic; the nitrogen carbene analogue also benefited the most from π-delocalization in all energetic analyses employed. Though the chalcogenium ions were found to contain the least amount of π-stabilization in the NBO energy analysis, they showed features characteristic of aromatic systems in both magnetic and orbital analyses.

4. The computational data obtained for **1-16** was used to assess the ability of different main group carbene analogues as σ-donors. The results suggest that, together with the parent carbene **5**, the boron and the aluminum systems display the best ligand properties. Totally different ligand behavior is expected for all chalcogenium dications as well as the stibenium ion due to the presence of two lone pairs of electrons around the divalent element in these systems.

5. The ability of different main group carbene analogues to act as π-acceptors was studied using arguments of frontier MO theory and an explanation for the chemical behavior observed for the heavier Group 14 and 15 species was given. Though all systems contain vacant π orbitals with appropriate characteristics with respect to backbonding, the Group 15 carbene analogues, which possess both relatively low-lying acceptor orbitals and an overall positive charge should display the

best internal π-acceptor ability. However, the π-acidity of systems **1-16** is naturally dependent on the metal to which the ligands bind to as well as on the overall charge of the formed complexes. Nevertheless, the results demonstrate that the extent of metal-to-ligand charge transfer can be affected by tuning the chemical composition of the ligand, thus allowing for example, the creation of carbene analogues with selective bonding capabilities towards different metal centers.

**Acknowledgement.** We thank the Academy of Finland, the University of Jyväskylä, the Natural Science and Engineering Research Council (NSERC) of Canada, the Ontario Ministry of Research and Innovation Early Researcher Award Program, the University of Western Ontario and the University of Calgary for their generous financial support.

**Supporting Information Available:** Figures of all valence orbitals of **1-16** are available free of charge at http://pubs.acs.org.

## References and Notes

[1] See, for example: (a) Herrmann, W. A.; Köcher, C. *Angew. Chem., Int. Ed. Engl.* **1997**, *36*, 2162. (b) Kühl, O. *Chem. Soc. Rev.*, **2007**, *36*, 592. (c) Nolan, S. P. (Ed.) *N-Heterocyclic Carbenes in Synthesis*; Wiley-VCH: Weinheim, 2006. (d) Glorius, F. (Ed) *N-Heterocyclic Carbenes in Transition Metal Catalysis. Topics in Organometallic Chemistry 21*; Springer: Berlin, Heidelberg, New York, 2007.

[2] (a) Arduengo, A. J. III; Harlow, R. L.; Kline M. *J. Am. Chem. Soc.* **1991**, *113*, 361. (b) Arduengo, A. J. III *Acc. Chem. Res.* **1999**, *32*, 913. (c) Arduengo, A. J. III; Krafczyk, R. *Chem. Unserer Zeit* **1998**, *32*, 6.

[3] See, for example: Herrmann, W. A. *Angew. Chem., Int. Ed.* **2002**, *41*, 1290.

[4] See, for example: Nair, V.; Bindu, S.; Sreekumar, V. *Angew. Chem., Int. Ed.* **2004**, *43*, 5130.

[5] Kascatan-Nebioglu, A.; Panzner, M. J.; Tessier, C. A.; Cannon, C. L.; Youngs, W. J. *Coord. Chem. Rev.* **2007**, *251*, 884

[6] Lee, C. K.; Chen, J. C. C.; Lee, K. M.; Liu, C. W.; Lin, I. J. B. *Chem. Mater.* **1999**, *11*, 1237.

[7] See, for example: (a) Arduengo, A. J. III; Goerlich, J. R.; Marshall, W. J. *J. Am. Chem. Soc.* **1995**, 117, 11027. (b) Hahn, F. E.; Le Van, D.; Paas, M.; Froehlich, R. *Dalton Trans.* **2006**, 860.

[8] Alder, R.W; Allen, P. R.; Murray, M.; Orpen, A. G. *Angew. Chem., Int. Ed. Engl.* **1996**, *35*, 1121.

[9] See, for example: (a) Alder, R. W.; Blake, M. E.; Bortolotti, C.; Bufali, S.; Butts, C. P.; Linehan, E.; Oliva, J. M.; Orpen, A. G.; Quayle, M. J. *Chem. Commun.* **1999**, 241. (b) Bazinet, R.; Yap, G. P. A.; Richeson, S. *J. Am. Chem. Soc.* **2003**, *125*, 13314. (c) Despagnet-Ayoub, E.; Grubbs, R. H. *J. Am. Chem. Soc.* **2004**, *126*, 10198. (d) Krahulic, K. E.; Enright, G. D.; Parvez, M.; Roeseler, R. *J. Am. Chem. Soc.* **2005**, *127*, 4142. (e) Präsang, C. Dnnadieu, B.; Betrand, G. *J. Am. Chem. Soc.* **2005**, *127*, 10182. (f) Scarborough, C. C.; Grady, M. J. W.; Guzei, I. A.; Gandhi, B. A.; Bunel, E. E.; Stahl, S. S. *Angew. Chem., Int. Ed.* **2004**, *44*, 5269. (g) Ishida, Y.; Donnadieu, B.; Bertrand, G. *P.N.A.S.* **2006**, *103*, 13585.

[10] Lavallo, V.; Canac Y.; Donnadieu, B.; Schoeller, W.W.; Bertrand, G. *Science* **2006**, *312*, 722.

[11] (a) Segawa, Y.; Yamashita, M.; Nozaki, K. *Science* **2006**, *314*, 113. (b) Schmidt, E. S.; Jockisch, A.; Schmidbauer, H. *J. Am. Chem. Soc.* **1999**, *121*, 9758. (c) Baker, R. J.; Farley, R. D.; Jones, C.; Kloth, C.; Murphy, D. D. *J. Chem. Soc., Dalton Trans.* **2002**, 3844. (d) Denk, M., Lennon, R.; Hayashi, R.; West, R.; Belyakov, A. V.; Verne, H. P.; Haaland, A.; Wagner, M.; Metzler, N. *J. Am. Chem. Soc* **1994**,116, 2691. (e) Herrmann, W. A.; Denk, M.; Behm, J.; Scherer, W.; Klingan, F.-R.; Bock, H.; Solouki, B.; Wagner, M. *Angew. Chem., Int. Ed. Engl.* **1992**, *31*, 1485. (f) Gans-Eichler, T.; Gudat, D.; Nieger, M. *Angew. Chem., Int. Ed.* **2002**, *41*, 1888. (g) Boche, G.; Andrews, P.; Harms, K.; Marsch, M.; Rangappa, K. S.; Schimeczek, M.; Willeke, C. *J. Am. Chem. Soc.* **1996**, *118*, 4925. (h) Denk, M. K.; Gupta, S.; Ramachandran, R. *Tetrahedron Lett.* **1996**, *37*, 9025. (i) Carmalt, C. J.; Lomeli, V.; McBurnett, B. G.; Cowley, A. H. *Chem. Commun.* **1997**, 2095. (j) Gudat, D.; Gans-Eichler, T.; Nieger, M. *Chem. Commun.* **2004**, 2434. (k) Dutton, J. L.; Tuononen, H. M. Jennings, M. C.; Ragogna, P. J. *J. Am. Chem. Soc.* **2006**, *128*, 12624.

[12] For some recent examples, see: (a) Chun-Liang, L.; Wen-Hsin, G.; Ming-Tsung, L.; Ching-Han., H. *J. Organomet. Chem.* **2005**, *690*, 5867. (b) Tafipolsky, M.; Scherer, W.; Öfele, K.; Artus, G.; Pedersen, B.; Herrmann, W. A.; McGrady, G. S. *J. Am. Chem. Soc.* **2002**, *124*, 5865. (c) Lord, R. L.; Wang, H.; Vieweger, M.; Baik, M.-H. *J. Organomet. Chem.* **2006**, *691*, 5505.

[13] For some recent examples, see: (a) Jacobsen, H.; Correa, A.; Costable, C.; Cavallo, L. *J. Organomet. Chem.* **2006**, *691*, 4350. (b) Gagliardi, L.; Cramer, C. J. *Inorg. Chem.* **2006**, *45*, 9442. Baba, E.; Cundari, T. R.; Firkin, I. *Inorg. Chim. Acta* **2005**, *358*, 2867. (c) Dorta, R.; Stevens, E. D.; Scott, N. M.; Costabile, C.; Cavallo, L.; Hoff, C. D.; Nolan,

S. P. *J. Am. Chem. Soc.* **2005**, *127*, 2485. (d) Frenking, G.; Solá, M.; Vyboishchikov, S. F. *J. Organomet. Chem.* **2005**, *690*, 6178.

[14] (a) Dixon, D. A.; Arduengo, A. J. III *J. Phys. Chem.* **1991**, *95*, 4180. (b) Cioslowski, J. *Int. J. Quantum Chem.* **1993**, *27*, 309. (c) Arduengo, A. J. III; Dias, H. V. R.; Dixon, D. A.; Harlow, R. L.; Klooster, W. T. Koetzle, T. F. *J. Am. Chem. Soc.* **1994**, *116*, 6812.

[15] (a) Heinemann, T. M.; Apeloig, Y.; Schwarz, H.; *J. Am. Chem. Soc.* **1996**, *118*, 2023. (b) Boehme, C.; Frenking, G. *J. Am. Chem. Soc.* **1996**, *118*, 2039.

[16] See, for example: (a) Heinemann, C.; Herrman, W. A.; Thiel, W. *J. Organomet. Chem.* **1994**, *475*, 73. (b) Arduengo, A. J. III; Bock, H.; Chen, H.; Denk, M.; Dixon, D. A.; Green, J. C.; Herrmann, W. A.; Jones, N. L.; Wagner, M.; West, R. *J. Am. Chem. Soc.* **1994**, *116*, 6641. (c) Lehmann, J. F.; Urquhart, S. G.; Ennis, L. E.; Hitchcock, A. P.; Hatano, K.; Gupta, S.; Denk, M. K. *Organometallics* **1999**, *18*, 1862. (d) Dhiman, A.; Mueller, T.; West, R.; Becker, J. Y. *Organometallics* **2004**, *23*, 5689. (e) West, R.; Buffy, J. J.; Haaf, M.; Mueller, T.; Gehrhus, B.; Lappert, M. F.; Apeloig, Y. *J. Am. Chem. Soc.* **1998**, *120*, 1639.

[17] See, for example: (a) Denk, M. K.; Gupta, S.; Lough, A. J. *Eur. J. Inorg. Chem.* **1999**, 41. (b) Gudat, D. *Eur. J. Inorg. Chem.* **1998**, 1087. (c) Gudat, D.; Haghverdi, A.; Hupfer, H.; Nieger, M. *Chem. Eur. J.* **2000**, *6*, 3414. (d) Burck, S.; Daniels, J.; Gans-Eichler, T.; Gudat, D.; Nättinen, K.; Nieger, M. *Z. Anorg. Allg. Chem.* **2005**, *631*, 1403.

[18] (a) Sundermann, A.; Reiher, M.; Schoeller, W. W. *Eur. J. Inorg. Chem.* **1998**, 305. (b) Metzler-Nolte, N. *New J. Chem.* **1998**, 793.

[19] (a) Perdew, J. P.; Burke, K.; Ernzerhof, M. *Phys. Rev. Lett.* **1996**, *77*, 3865. (b) Perdew, J. P.; Burke, K.; Ernzerhof, M. *Phys. Rev. Lett.* **1997**, *78*, 1396. (c) Perdew, J. P.; Ernzerhof, M.; Burke, K. *J. Chem. Phys.* **1996,** *105*, 9982. (d) Ernzerhof, M.; Scuseria, G. E. *J. Chem. Phys.* **1999**, *110*, 5029.

[20] (a) The TZVP basis sets were used as they are referenced in the Turbomole 5.9 internal basis set library. See ftp://ftp.chemie.uni-karlsruhe.de/pub/ for explicit basis set listings. (b) Bergner, A.; Dolg, M.; Kuechle, W.; Stoll, H.; Preuss, H. *Mol. Phys.* **1993**, *80*, 1431.

[21] Frisch, M. J. *et al.* Gaussian 03, (Revision C.02), Gaussian, Inc., Pittsburgh, PA, 2003.

[22] Glendening, E.D.; Badenhoop, J. K.; Reed, A. E.; Carpenter, J. E.; Bohmann, J. A.; Morales, C. M.; Weinhold, F. NBO 5.0, Theoretical Chemistry Institute, University of Wisconsin, Madison, WI, 2001.

[23] Noury, S.; Krokidis, X.; Fuster, F.; Silvi, B. TopMoD, Universite Pierre et Marie Curie, Paris, France, 1997.

[24] Bader, R. W. F.; Krugg,, P., AIMPAC, Department of Chemistry, McMaster University, Hamilton, ON, Canada, 1990.

[25] Leites, L. A.; Bukalov, S. S.; Zabula, A. V.; Garbuzova, I. A.; Moser, D. F.; West, R. *J. Am. Chem. Soc.* **2004**, *126*, 4114.

[26] (a) Reed, A. E.; Weinhold, F. J. *Chem. Phys.* **1983**, *78*, 4066. (b) Reed, A. E.; Weinstock, R. B.; Weinhod, F. J. *J. Chem. Phys.* **1985**, *83*, 735. (c) Foster, J. P.; Weinhold, F. *J. Am. Chem. Soc.* **1980**, *102*, 7211. (d) Reed, A. E.; Curtiss, L. A.; Weinhold, F. *Chem. Rev.* **1988**, *88*, 899.

[27] Sannigrahi, A. B.; Nandi, P. K.; Schleyer, P. v. R. *Chem. Phys. Lett.* **1993**, *204*, 73.

[28] Such comparison is justified as both constructs are merely different representations of the same π-electron density.

[29] (a) Ettel, F.; Huttner, G.; Zsolnai, L. *Angew. Chem., Int. Ed. Engl.* **1989**, *28*, 1496. (b) Ettel, F.; Huttner, G.; Imhof, W. *J. Organomet. Chem.* **1990**, *397*, 299.

[30] Although the "π-charge" associated to the dicoordinate group 14 element in the $\pi_3$ orbital does in fact increase down the group, the σ-density and the electron density in the $\pi_1$ orbital become depleted. As a consequence, the calculated atomic charges for elements E become more positive when going down the group, which is in agreement with their electronegativities. Hence, the chelated atom model is not in contradiction with the relative oxidation strengths of the Group 14 elements.[15b]

[31] This was confirmed by running natural resonance theory (NRT) analyses for the systems in question.

[32] Gans-Eichler, T.; Gudat, D.; Nättinen, K.; Nieger, M. *Chem. Eur. J.* **2006**, *12*, 1162.

[33] The chelated atom model **I** was supported by experimental observations which showed that a tin atom from a diazastannole **8** can be transferred to a free diazadiene.[11f] NMR data indicated that the exchange process proceeds without participation of further detectable intermediates and the reaction was expected to follow an associative mechanism. However, such mechanism seems unlikely if the chelated atom resonance structure **I** has a significant contribution in the wave function of free **8** as the initial reaction step would involve a coordination of a free diazadiene ligand to a tetrahedral Sn centre with two lone pairs and two dative SnN bonds. In addition, the geometries of the geometry optimized $C_1$ symmetric transition states are not in agreement with such description.[32] There are two other important facts which further support the view that **8** could equally well be described as a Sn(II) species.[32] (i) Metathesis reactions have later been observed for the analogous germylenes, which indicates that the easy cheletropic fragmentation observed for **8** does not require a difference in its electronic structure as compared to lighter Group 14 homologues. (ii) It has been demonstrated that in the case of tin systems, the energy hypersurface for the spirocyclic

intermediate in the metathesis reaction has biradical character, which readily explains the instability of the spirocyclic addition product and the facile nature of the tin transfer reaction.

[34] The Ge-bipyridyl complex was subjected to ELF analysis which supports this description. When compared to results obtained for **7**, a decrease in *V*(CC) and *V*(EN) populations is observed, which is accompanied by an increase in *V*(NC) and, in particular, *V*(E) populations. Hence, according to ELF analysis, the electronic structure of the Ge-bipyridyl system is significantly more polarized towards the chelated atom model than **7**.

[35] Fürstner, A.; Krause, H.; Lehmann, C. W. *Chem. Commun.* **2001**, 2372.

[36] It should, however, be noted that NAOs are intrinsic to the wave function, rather than to a particular choice of basis functions, and converge to well defined limits as the quality wave function is improved. Therefore, although NPA and NBO analyses are formulated using the language of orbitals, the results obtained are at least independent of the form of the starting basis *i.e.* canonical MOs, Kohn-Sham orbitals, localized orbitals, plane waves, etc.

[37] (a) Biegler-Koenig, F. W.; Nguyen-Dang, T. T.; Tal, Y.; Bader, R. F. W.; Duke, A. J. J. Phys. B: At. Mol. Phys. **1981**, *14*, 2739. (b) Bader, R. F. W.; Nguyen-Dang, T. T. *Adv. Quant. Chem.* **1981**, *14*, 63.

[38] (a) Silvi, B.; Savin, A. *Nature* **1994**, *371*, 683. (b) Savin, A.; Becke, A. D.; Flad, J.; Nesper, R.; Preuss, H.; Schnering, H. G. *Angew. Chem., Int. Ed. Engl.* **1991**, *30*, 409. (c) Savin, A.; Nesper, R.; Wengert, S.; Fässler, T. F. *Angew. Chem., Int. Ed. Engl.* **1997**, *36*, 1809.

[39] Average basin populations listed in Table 5 can be compared with the values 2.9 and 2.2 determined for the *V*(NC) and *V*(CC) basins, respectively, of the free *cis*-DAB ligand.

[40] See, for example: (a) Katritzky, A. R.; Karelson, M.; Sild, S.; Krygowski, T. M.; Jug, K. *J. Org. Chem.* **1998**, *63*, 5228. (b) Cyrañski, M. K.; Krygowski, T. M.; Katritzky, A. R.; Schleyer, P. v. R. *J. Org. Chem.* **2002**, *67*, 1333.

[41] All reaction energies are calculated using $^1A_1$ ground state for $:EH_2$.

[42] The NBO derived delocalization energies for the stibenium cation **12** are 366 and 321 kJ $mol^{-1}$ when its electronic structure is compared to the perfectly C=C and C=N double bonded Lewis structures, respectively. Hence, the close agreement between the two numbers confirms that both Lewis structures make an important contribution to its electronic structure.

[43] (a) Schleyer, P. v. R.; Maerker, C.; Dransfeld, A.; Jiao, H.; van Eikema Hommes, N. J. R. *J. Am. Chem. Soc.* **1996**, *118*, 6317. (b) Chen, Z.; Wannere, C. S.; Corminboef, C.; Puchta, R.; Schleyer, P. v. R. *Chem. Rev.* **2005**, *105*, 3842. (c) Fallah-Bagher-Shaidaei, H.; Wannere, C. S.; Corminboeuf, C.; Puchta, R.; Schleyer, P. v. R. *Org. Lett.* **2006**, *8*, 863.

[44] (a) Baker, R. J.; Jones, C.; Platts, J. A. *Dalton Trans.* **2003**, 3673. (b) Baker, R. J.; Jones, C.; Platts, J. A. *J. Am. Chem. Soc.* **2003**, *125I*, 10534. (c) Rupar, P. A.; Jennings M. C.; Baines, K. M. *Can. J. Chem.* **2007**, *85*, 141. (d) Jones. C.; Mills, D. P.; Rose, R. P. *J. Organomet. Chem.* **2006**, *691*, 3060. (e) Aldridge, S.; Baker, R. J.; Coombs, N. D.; Jones, C.; Rose, R. P.; Rossin, A.; Willock, D. J. *Dalton. Trans.* **2006**, 3313.

[45] (a) Frenking, G.; Solà, M.; Vyboishchikov, S. F. *J. Organomet. Chem.* **2005**, *690*, 6178. (b) Yongjun, X. H.; Gantzel, P.; Meyer, K. *Organometallics* **2003**, *22*, 612. (c) Jacobsen, H.; Correa, A.; Costabile, C.; Cavallo, L. *J. Organomet. Chem.* **2006**, *691*, 4350.

[46] Gudat, D.; Haghverdi, A.; Nieger, M. *J. Organomet. Chem.* **2001**, *617*, 383.

[47] Boehme, C.; Frenking, G. *Organometallics* **1998**, *17*, 5801.